RSC Advances

PAPER

View Article Online
View Journal | View Issue

Cite this: *RSC Adv.*, 2022, **12**, 25204

Novel quinoxaline derivatives as dual EGFR and COX-2 inhibitors: synthesis, molecular docking and biological evaluation as potential anticancer and anti-inflammatory agents†

Eman A. Ahmed,[a] Mamdouh F. A. Mohamed *[b] and Omran A. Omran[a]

Novel quinoxaline derivatives (**2a–d**, **3**, **4a**, **4b** and **5–15**) have been synthesized *via* the reaction of 4-methyl-3-oxo-3,4-dihydroquinoxaline-2-carbohydrazide (**1**) with different aldehydes, ketones, diketones, ketoesters, as well as hydrazine, phenyl isothiocyanate, carbon disulphide. The synthesized products have been screened for their *in vitro* anticancer and COX inhibitory activities. Most of the synthesized compounds exhibited good anticancer and COX-2 inhibitory activities. MTT assay revealed that compounds **11** and **13** were the most potent and exhibited very strong anticancer activity against the three cancer cell lines with IC_{50} values ranging from 0.81 μM to 2.91 μM. Compounds **4a** and **5** come next and displayed strong anticancer activity against the three cancer cell lines with IC_{50} values ranging from 3.21 μM to 4.54 μM. Mechanistically, compounds **4a** and **13** were the most active and potently inhibited EGFR with IC_{50} = 0.3 and 0.4 μM, respectively. Compounds **11** and **5** come next with IC_{50} = 0.6 and 0.9 μM, respectively. Moreover, compounds **11** and **13** were the most potent as COX-2 inhibitors and displayed higher potency against COX-2 (IC_{50} = 0.62 and 0.46 μM, respectively) more than COX-1 (IC_{50} = 37.96 and 30.41 μM, respectively) with selectivity indexes (SI) of 61.23 and 66.11, respectively. Compounds **4a** and **5** comes next with IC_{50} = 1.17 and 0.83 μM and SI of 24.61 and 48.58, respectively. Molecular docking studies into the catalytic binding pocket of both protein receptors, EGFR and COX-2, showed good correlation with the obtained biological results. Parameters of Lipinski's rule of five and Veber's standard were calculated and revealed that compounds **4a**, **5**, **11** and **13** had a reasonable drug-likeness with acceptable physicochemical properties. Therefore, based on the obtained biological results accompanied with the docking study and physicochemical parameters, it could be concluded that compounds **4a**, **5**, **11** and **13** could be used as promising orally absorbed dual anti-inflammatory agents *via* inhibition of COX-2 enzyme and anticancer candidates *via* inhibition of EGFR enzyme and could be used as a future template for further investigations.

Received 20th July 2022
Accepted 30th August 2022

DOI: 10.1039/d2ra04498f

rsc.li/rsc-advances

1. Introduction

Cancer, with 7–10 million human mortalities annually worldwide, is still rising at an alarm rate as one of the most intractable diseases globally.[1–3] It is a complex, heterogeneous, multigenic disease and is the leading cause of death preceded only by heart disease.[4,5] There are many cancer hallmarks, tumor-promoting inflammation is now well-recognized as one of the cancer hallmarks. Moreover, both acute and chronic inflammatory processes have a significant influence on the development and growth of cancer.[6–8] Recent evidence has expanded that inflammation is not only a vital component of tumor progression but it is also predisposing to the development of cancer and facilitates all stages of tumorigenesis.[9] Till now, there are more than one hundred cancer types; each one needs unique diagnosis and treatment.[2] Indeed, there are many effective anticancer drugs currently available on the market, such as the traditional anticancer chemotherapeutic agents that prevent cell division and replication of DNA. Unfortunately, most of these drugs lack selectivity and specificity, leading to issues such as the common severe adverse effects.[2,10] Thus, there is an urgent necessity for the innovation and discovery of novel small molecules with potential to be effective as potent and selective anticancer agents which still represents a major challenge to medicinal chemists.[2]

Currently, it is estimated that inflammatory reactions are responsible for up to 15–20% of cancer-related deaths.[11] Additionally, administration of non-steroidal, anti-inflammatory drugs is connected with a lower risk of developing numerous tumors and decreased mortality further underlining the role of

[a]*Department of Chemistry, Faculty of Science, Sohag University, Sohag 82524, Egypt*
[b]*Department of Pharmaceutical Chemistry, Faculty of Pharmacy, Sohag University, 82524 Sohag, Egypt. E-mail: mamdouhfawzy3@yahoo.com; mamdouh.fawzi@pharm.sohag.edu.eg; Tel: (+20)-01018384461*

† Electronic supplementary information (ESI) available. See https://doi.org/10.1039/d2ra04498f

inflammation in neoplastic transformation.[12] Nonsteroidal anti-inflammatory drugs (NSAIDs) are among the most commonly prescribed medication worldwide for the treatment of both acute and chronic inflammation,[13] fever, pain[14] and inflammation-related disorders.[15] However, the long-term usage of non-selective NSAIDs has a number of undesirable side effects, including nephrotoxicity, hepatotoxicity, gastrointestinal irritation, bleeding and ulceration.[16,17] Several methods have been reported for improving non-selective NSAIDs.[18,19] One strategy is there placement of the acidic carboxylic functional groups in NSAIDs with alternative less acidic heterocyclic bioisosteres. Another strategy is the synthesis of selective COX-2 inhibitors as a new generation of NSAIDs, which would preserve the anti-inflammatory effectiveness while reducing gastric toxicity. Also, development of dual COX and LOX inhibitors with moderate selectivity towards COX-2 at micromole level.[20] Recently, the more promising strategy through the development of NSAIDs/iNOS inhibitors for the treatment of inflammatory diseases by decreasing the over production of PGE_2 and NO, respectively.[17,21–23]

Finally, Mantovani classified cancer-related inflammation into two pathways: (i) the intrinsic pathway, which is linked to genetic events that trigger inflammation and neoplastic transformation, and (ii) the extrinsic pathway, which explains inflammatory conditions that promote carcinogenesis. Based upon these observations, it has been proposed that cancer-related inflammation (CRI) might be considered as the "seventh hallmark" of cancer.[24] Accordingly, the development of dual acting anti-inflammatory/anticancer candidates is urgently needed and represents a promising approach in treatment of both cancer and inflammatory diseases.

Over the years and due to their significant role in the drug design, development and discovery, nitrogen-based heterocycles have attracted considerable attention.[25] Among the N-containing heterocyclic pharmacophores; quinoxaline moiety represents an important class of heterocyclic compounds due to their significant physiological properties and promising applications in medicinal chemistry.[26] Notably, many approved drugs such as the antibiotics echinomycin, levomycin, and actinoleutin have quinoxaline as part of their structure.[27] Moreover, quinoxaline moiety and its derivatives have received significant attention due to their wide spectrum of pharmaceutical and biological properties such as, among other insecticidal, antidepressant, antifungal, anticonvulsant, anthelmintic, anti-inflammatory, antiviral, antimalarial,antibacterial, antiprotozoal, and anticancer.[26,28–30] CQS (4-amino-*N*-(5-chloroquinoxalin-2-yl) benzenesulfonamide, NSC 339004)[31,32] and XK469 (2-[4-(7-chloroquinoxalin-2-yl) oxyphenoxy]propanoic acid, NSC 697887)[33,34] are examples of potent anticancer quinoxalines. Moreover, these compounds have been widely used in technology as dyes, chemical switches, electroluminescent materials, photo-initiators, cavitands and organic semiconductors.[26,28,29,35]

On the other hand, hydrazones are found in numerous of the bioactive heterocyclic compounds that are of very important use because of their several biological and clinical medicinal applications.[36,37] Hydrazone derivatives of heteroaromatic compounds have been proved to have, among other, antidepressant, antifungal, antimicrobial, antitubercular, anticonvulsant, analgesic, anti-inflammatory, antimalarial, antiplatelet, cardio protective and antiviral with anticancer activities being of significant interest.[3,36,37]

Motivated by the aforementioned facts and with the hope of yielding more potent, less toxic, selective, and effective dual acting anti-inflammatory/anticancer candidates, the main aim of this work is to synthesize a new series of quinoxaline-hydrazone derivatives as depicted in Fig. 1 and Scheme 1. Additionally, various substituents attached to the quinoxaline

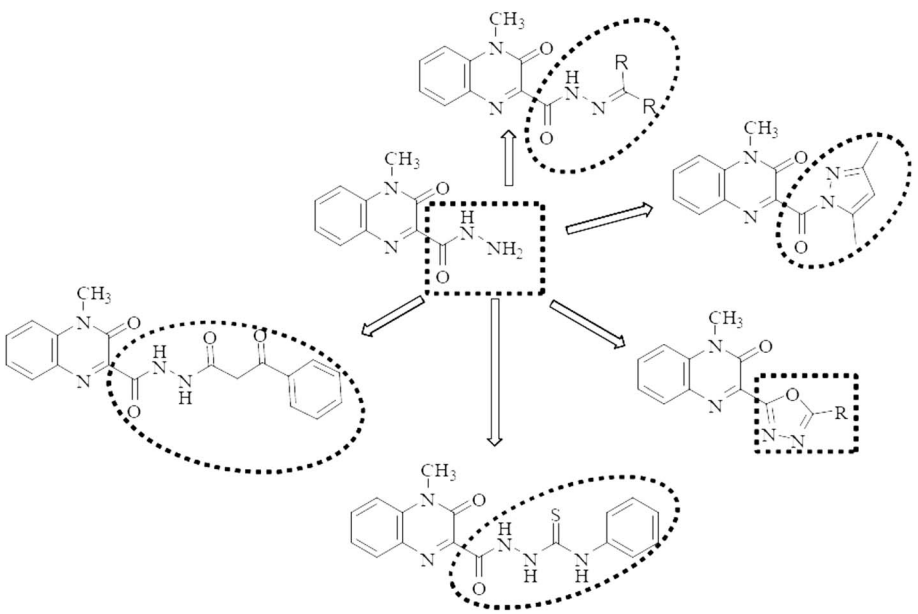

Fig. 1 Rationale design of quinoxaline derivatives as anticancer/anti-inflammatory agents.

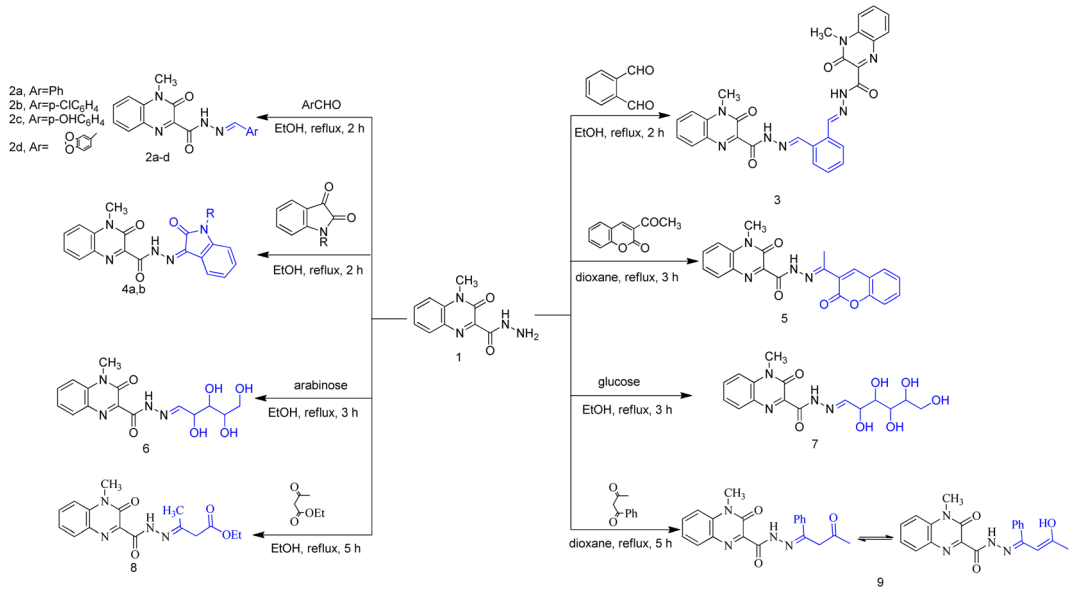

Scheme 1 Synthesis of compounds **2–9**.

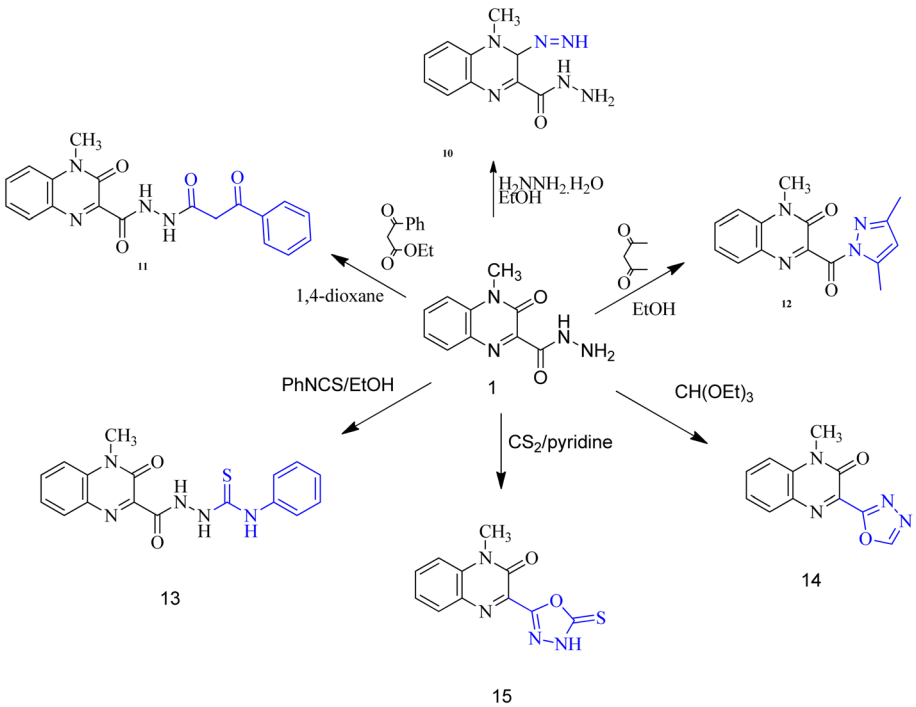

Scheme 2 Synthesis of compounds **10–16**.

scaffold such as five membered rings (pyrazole and 1,3,4-oxadiazole), hydrazide or thiocarbohydrazide (Fig. 1 and Scheme 2) to investigate their anticancer activity as well as their EGFR, COX-1 and COX-2 inhibitory activities and study their structure activity relationship. Docking study, finally, will be carried out to investigate the binding interactions of the most potent compounds into the pocket of EGFR and COX-2 receptor proteins.

2. Results and discussion

2.1. Chemistry

Heterocycles, such as coumarin, oxindole among others, are highly valuable structures in medicinal chemistry and they represent ubiquitous fragments of several natural products, pharmaceuticals and designed bioactive drug candidates.[38–40] Therefore, and in continuation of our work,[41] we reported here

synthesis of some novel molecules which have quinoxaline moiety coupled to N- or O-heterocyclic ring through acetyl/amide linkage as illustrated in Scheme 1 and 2. The 4-methyl-3-oxo-3,4-dihydroquinoxaline-2-carbohydrazide (**1**) was prepared according to our reported method,[41] *via* the treatment of ethyl 4-methyl-3-oxo-3,4-dihydroquinoxaline-2-carboxylate with hydrazine hydrate. Carbohydrazide **1** was allowed to react with different aromatic aldehydes such as benzaldehyde, *p*-chlorobenzaldehyde, *p*-hydroxybenzaldehyde, and piperonlaldehyde to afford the corresponding *N*′-arylidene-4-methyl-3-oxo-3,4-dihydroquinoxaline-2-carbohydrazide **2a–d**, a mixture of keto- and enol-isomers of Schiff base was obtained in each case.

The structure of compounds **2a–d** was established on the basis of their spectral and analytical data. Their IR spectra showed the absence of absorption bands corresponding to $NHNH_2$ groups and revealed a new absorption band at 3173–3111 cm^{-1} assignable to NH groups. Also, their ^{1}H-NMR spectra showed the disappearance of the signal corresponding to NH_2 group and exhibited a signal at δ 12.47–12.03 and 8.35–7.88 ppm due to presence of NH and azomethine protons, respectively, as well as increasing of aromatic protons. In addition, when compound **1** was subjected to react with dialdehyde such as *o*-phthaldehyde, the bis Schiff base *N*′,*N*″-(1,2-phenylenebis(methan-1-yl-1-ylidene))bis(4-methyl-3-oxo-3,4-dihydroquinoxaline-2-carbohydrazide) **3** were formed. The structure of compound **3** has been approved by disappearance of the absorption bands at 1700 cm^{-1} corresponding to formyl group. Also, ^{1}H-NMR revealed that the ratio between aromatic and methyl protons is 2 : 1 in agreement with the desired structure. Compound **1** was then reacted with biologically active heterocyclic ketones such as isatin and acetyl coumarin. Thus, treatment with isatin and/or *N*-methyl isatin in boiling ethanol, gave 4-methyl-3-oxo-*N*′-(2-oxoindolin-3-ylidene)-3,4-dihydroquinoxaline-2-carbohydrazide **4a** and/or 4-methyl-*N*′-(1-methyl-2-oxoindolin-3-ylidene)-3-oxo-3,4-dihydroquinoxaline-2-carbohydrazide **4b**, respectively. Similarly, when acetyl coumarin was reacted with compound **1** in boiling dioxane, afforded 4-methyl-3-oxo-*N*′-(1-(2-oxo-2*H*-chromen-3-yl)ethylidene)-3,4-dihydroquinoxaline-2-carbohydrazide **5**. IR spectra of compounds **4a**, **4b** and **5** showed new absorption bands at 1702 + 3 for the carbonyl of isatines or coumarin, in addition to an absorption band at 3438 corresponding to the new NH in the case of compound **4a**. Also, ^{1}H-NMR revealed a new signal at 10.93 due to the new NH in the case of compound **4a** and new signals at 3.24 and 2.29 due to the new CH_3 in the case of compounds **4b** and **5**, respectively. Condensation of compound **1** with two different aldoses, arabinose as an aldopentose and/or glucose as an aldohexose has been carried out to produce the polyhydroxyalkylidene quinoxaline carbohydrazide derivatives, 4-methyl-3-oxo-*N*′-(2,3,4,5-tetrahydroxypentylidene)-3,4-dihydroquinoxaline-2-carbohydrazide (**6**) and/or 4-methyl-3-oxo-*N*′-(2,3,4,5,6-pentahydroxyhexylidene)-3,4-dihydroquinoxaline-2-carbohydrazide (**7**), respectively. In the IR spectra, a series of absorption bands were observed at 3456, 3395, 3338, 3303 or at 3570, 3441, 3388, 3366, 3258 corresponding to hydroxy groups in the case of compounds **6** or **7**, respectively.

When carbohydrazide **1** was reacted with ethyl acetoacetate and/or benzoyl acetone, open-chain products formed. Reaction with ethyl acetoacetate in boiling ethanol gave ethyl 3-(2-(4-methyl-3-oxo-3,4-dihydroquinoxaline-2-carbonyl)hydrazono) butanoate (**8**), the ^{1}H NMR spectrum exhibited singlet signal at δ 11.6 ppm which was exchangeable with deuterium on addition of deuterium oxide and was assigned to N–H proton, new two signals were observed at 3.46 and 1.99 ppm for methylene and methyl protons, respectively, in addition to two sets of signals distinguish the presence of ethoxy group (OCH_2CH_3) at 4.16 and 1.26 ppm. The product was formed by nucleophilic addition of the amino group of **1** to the carbonyl acetyl group followed by elimination of water. Also, reaction of benzoylacetone with **1** in boiling dioxane, led to (*Z*)-4-methyl-3-oxo-*N*′-(3-oxo-1-phenylbutylidene)-3,4-dihydroquinoxaline-2-carbohydrazide (**9**). Compound **1** was allowed to react with hydrazine hydrate in boiling ethanol. The product of the reaction was proved as 3-diazenyl-4-methyl-3,4-dihydroquinoxaline-2-carbohydrazide (**10**) by spectral and analytical data. IR spectrum showed the presence of absorption bands corresponding to NH_2; 2NH and CO groups, also, ^{1}H-NMR revealed new four signals at 9.42, 4.43, 4.34 and 3.39 ppm due to 2NH; NH_2 and CH protons.

Whereas, reaction of ethyl benzoylacetate with **1** in boiling dioxane, led to 4-methyl-3-oxo-*N*′-(3-oxo-3-phenylpropanoyl)-3,4-dihydroquinoxaline-2-carbohydrazide (**11**), the product was formed by nucleophilic addition of the amino group of **1** to the carbonyl ester group followed by elimination of ethanol molecule. On the other hand, upon heating the carbohydrazide **1** with acetylacetone in ethanol, the *N*-pyrazolo derivative was formed. Compound **12** showed in its ^{1}H-NMR spectrum, new three singlet signals at 6.07, 2.72, 2.16 ppm due to 4-H pyrazole, two methyl protons at 5 and 3 positions of pyrazole moiety. In addition, the carbohydrazide **1** was allowed to react with phenyl isothiocyanate in boiling ethanol, to give 2-(4-methyl-3-oxo-3,4-dihydroquinoxaline-2-carbonyl)-*N*-phenylhydrazine-carbothioamide (**13**). Also, oxadiazole derivative **14** was formed from interaction of **1** with triethyl orthoformate. The ^{1}H-NMR spectrum showed disappearance of signals related to NH and NH_2 groups, and appearance of new signal due to CH proton of new oxadiazole ring. Finally, the interaction of **1** with carbon disulfide in boiling pyridine afforded 3-(5-mercapto-1,3,4-oxadiazol-2-yl)-1-methylquinoxalin-2(1*H*)-one (**15**). The spectral data of compound **15** are coincident with the suggested structure.

2.2. Biological evaluation

2.2.1. Anticancer evaluation. All the newly synthesized 18 quinoxaline derivatives were screened for their *in vitro* anticancer activity against three cancer cell lines; breast (MCF-7), liver (HepG2) and colon (HCT-116) carcinoma cell lines, at a single concentration of 10 μM. The obtained results were presented as percentage growth inhibition (GI%), (Table 1). The obtained results of tested compounds **2a–d**, **3**, **4a**, **4b**, **5–15** revealed that most compounds displayed a good anticancer activity. Among them, compounds **2c**, **4a**, **5**, **8**, **9**, **11** and **13** were found to be the most active and they displayed a remarkable anticancer activity (≥88.68% growth inhibition) against the

Table 1 Cell growth inhibition (GI% at 10 μM) of the target compounds against MCF-7, HepG2 and HCT-116 cancer cell lines

	MCF-7	HepG2	HCT-116
2a	82.85 ± 0.49	89.21 ± 0.63	69.25 ± 0.45
2b	95.46 ± 1.25	90.76 ± 0.29	88.68 ± 0.52
2c	69.72 ± 0.46	77.95 ± 0.56	61.92 ± 0.55
2d	50.14 ± 0.46	56.95 ± 0.35	59.47 ± 0.78
3	46.52 ± 1.12	54.25 ± 0.60	63.79 ± 0.44
4a	90.14 ± 0.76	91.82 ± 0.35	92.79 ± 0.15
4b	61.47 ± 0.37	52.35 ± 0.74	59.46 ± 0.27
5	91.47 ± 0.25	90.79 ± 0.21	93.75 ± 0.29
6	10.82 ± 0.76	21.38 ± 0.52	41.79 ± 1.27
7	10.32 ± 0.48	26.37 ± 0.83	33.87 ± 1.27
8	95.96 ± 0.22	94.63 ± 0.35	96.42 ± 0.81
9	92.97 ± 0.54	96.83 ± 0.29	97.89 ± 0.69
10	49.76 ± 0.86	52.43 ± 0.69	86.63 ± 1.31
11	92.57 ± 0.43	92.78 ± 0.38	97.63 ± 0.16
12	33.47 ± 0.82	53.78 ± 1.38	49.22 ± 1.23
13	95.39 ± 0.27	96.75 ± 0.29	97.87 ± 0.19
14	29.27 ± 0.63	25.74 ± 1.67	33.34 ± 1.32
15	43.47 ± 0.63	59.47 ± 1.92	76.32 ± 1.22

three cancer cell lines. Ongoing through the details of the obtained results of compounds **2a–d**, it is obvious that introducing a withdrawing group as Cl (**2b**) resulted in increase in the activity against the three cancer cell lines. On the other hand, substitution with donating groups such as OH or dioxolyl group (**2c** and **2d**, respectively) led to significant decrease in the activity. Replacement of *N*′-benzylidene moiety with isatin (**4a**) significantly enhance the anticancer activity, while replacement with *N*-methylisatin (**4b**) led to significant decrease in the activity less than both**2a** and **4a**. Moreover, replacement of the *N*′-benzylidene moiety with 3-acetylcoumarine moiety as in (**5**) regained the anticancer activity against the three cancer cell lines. Shifting to tetrahydroxypentylidene (**6**), pentahydroxyhexylidene (**7**) or converting the 3-oxo to 3-diazenyl (**10**) resulted in a dramatic decrease in the anticancer activity. The obtained products *via* the reaction of compound **1** with ethylacetoacetate (**8**), benzoylacetone (**9**), ethyl benzoyl acetate (**11**), phenyl isothiocyanate (**13**), significantly improved the anticancer activity of these products against the three cancer lines. Finally, masking the hydrazide spacer *via* attachment of five membered ring either with C=O as spacer, as in compound **12** with pyrazole moiety, or directly to the quinoxaline scaffold as in compound **14** (1,3,4-oxadiazole) and compound **15** (1,3,4-oxadiazole-2-thione) again we noticed a dramatic decrease in the anticancer activity against the three cancer cell lines.

The most potent compounds **2b**, **4a**, **5**, **8**, **9**, **11** and **13** were further selected upon their 1st screening results for determination of their IC_{50} at 10-fold dilutions of five different concentrations (0.01, 0.1, 1, 10 and 100 μM) using doxorubicin as a reference drug. The obtained results, as shown in Table 2, revealed that the tested compounds showed variable results varying from very strong to moderate anticancer activity against the three used cancer cell lines. Among all, compounds **11** and **13** were the most potent and exhibited very strong anticancer activity against the three cancer cell lines with IC_{50} values

Table 2 Anticancer activity (IC_{50} μM) of compounds **2b**, **4a**, **5**, **8**, **9**, **11**, **13** and doxorubicin against MCF-7, HepG2 and HCT-116 cancer cell lines

Compounds	MCF-7	HepG2	HCT-116
2b	15.98 ± 0.06	12.41 ± 0.05	16.32 ± 0.24
4a	4.42 ± 0.12	4.23 ± 0.09	4.54 ± 0.19
5	3.21 ± 0.10	3.62 ± 0.21	3.46 ± 0.15
8	10.50 ± 0.14	13.82 ± 0.06	12.97 ± 0.08
9	6.84 ± 0.07	5.54 ± 0.27	8.75 ± 0.25
11	2.91 ± 0.23	2.41 ± 0.07	2.38 ± 0.26
13	0.81 ± 0.13	0.96 ± 0.09	1.12 ± 0.19
Doxorubicin	0.90 ± 0.02	1.21 ± 0.08	0.51 ± 0.03

ranging from 0.81 μM to 2.91 μM. Compounds **4a** and **5** come next and displayed strong anticancer activity against the three cancer cell lines with IC_{50} values ranging from 3.21 μM to 4.54 μM. Compound **9** showed good anticancer activity with IC_{50} values 6.84, 5.54 and 8.75 μM against MCF-7, HepG2 and HCT-116, respectively. Finally, compounds **2b** and **8** exhibited moderate anticancer activity against the three cancer lines with IC_{50} values more than 10 μM as illustrated in Table 2. From these results, it could be concluded that compounds **4a**, **5**, **11** and **13** could be considered as promising anticancer candidates.

2.2.2. ***In vitro* cyclooxygenase (COX) inhibition assay.** The most potent anticancer compounds **2b**, **4a**, **5**, **8**, **9**, **11** and **13** were subjected to cyclooxygenase (COX) inhibition assay to determine the ability of these newly synthesized quinoxaline derivatives to inhibit both bovine COX-1 and COX-2 using a colorimetric enzyme immune assay (EIA) kit. Moreover, selectivity indexes (SI values) against COX-2 were calculated as IC_{50} (COX-1)/IC_{50} (COX-2) and compared with celecoxib as a positive control and a standard drug. As illustrated in Table 3, compounds **11**, **13** were the most potent and displayed good inhibitory activities against COX-2 (IC_{50} = 0.62 and 0.46 μM, respectively) more than COX-1 (IC_{50} = 37.96 and 30.41 μM, respectively) with selectivity indexes (SI) of 61.23 and 66.11, respectively. Compound **5** comes next with IC_{50} = 0.83 μM and SI of 48.58. Finally, compounds **4a** and **9** were the least active with IC_{50} values equal to 1.17 and 2.21 μM and SI of 24.61 and 17.52, respectively. On the other hand, compounds **2b** and **8**

Table 3 *In vitro* COX-1, COX-2 and EGFR inhibitory activity (IC_{50} μM) of the most potent compounds

Compounds	COX-1	COX-2	SI	EGFR
2b	4.42 ± 1.67	5.26 ± 0.49	0.84	—
4a	28.79 ± 1.02	1.17 ± 0.15	24.61	0.3 ± 0.01
5	40.32 ± 3.35	0.83 ± 0.4	48.58	0.9 ± 0.01
8	1.62 ± 1.21	2.73 ± 0.04	0.59	—
9	38.72 ± 1.27	2.21 ± 0.14	17.52	—
11	37.96 ± 0.66	0.62 ± 0.07	61.23	0.6 ± 0.04
13	30.41 ± 1.63	0.46 ± 0.06	66.11	0.4 ± 0.02
Erlotinib	—	—	—	0.08 ± 0.03
Indomethacin	0.52 ± 0.02	0.84 ± 0.4	0.62	—
Celecoxib	29.49 ± 1.63	0.34 ± 0.06	86.74	—

were slightly selective towards COX-1 more than COX-2 with IC_{50} values equal to 4.42 and 1.62 μM, respectively. Based on these results, it could be concluded that compounds **4a**, **5**, **11**, **13** could be used as anti-inflammatory agents *via* inhibition of COX-2 enzyme.

2.2.3. *In vitro* EGFR-TK inhibition assay. To investigate a possible anticancer mechanism of the most potent compounds **4a**, **5**, **11** and **13**, EGFR-TK assay was carried out using erlotinib as a positive control as shown in Table 3. The results showed that compounds **4a** and **13** were the most active with IC_{50} = 0.3 and 0.4 μM, respectively. Compounds **11** comes next with IC_{50} = 0.6 μM. Finally, compound **5** was the least active with IC_{50} = 0.9 μM. These results revealed that these compounds were potent EGFR inhibitors. Collectively, it could be concluded that compounds **4a**, **5**, **11**, **13** could be used as dual anti-inflammatory agents *via* inhibition of COX-2 enzyme and anticancer candidates *via* inhibition of EGFR enzyme.

3. Molecular docking studies

Docking studies have been carried out to elucidate the binding mode of compounds **13** and **11** as the most potent COX2 inhibitors and compounds **4a** and **13** as the most potent EGFR inhibitors with the target COX2 (PDB ID: 3LN1)[20,42] and **EGFR** (PDB ID: 1M17)[43,44] enzymes using Discovery Studio software package. Firstly, the validation step was carried out *via* redocking of the ligand on both used crystal structures and the RMSD values were found to be less than 2 which proved the validity of the produced docking results.

3.1. Molecular docking study of COX2 (PDB ID: 3LN1)

Analysis of the docking results of compound **13** revealed that it incorporated in the formation of six hydrogen bonds with Gln178, Leu338 (2 HB), Ser339 (2 HB) and Phe504 amino acid residues. In addition, compound **13** displayed several

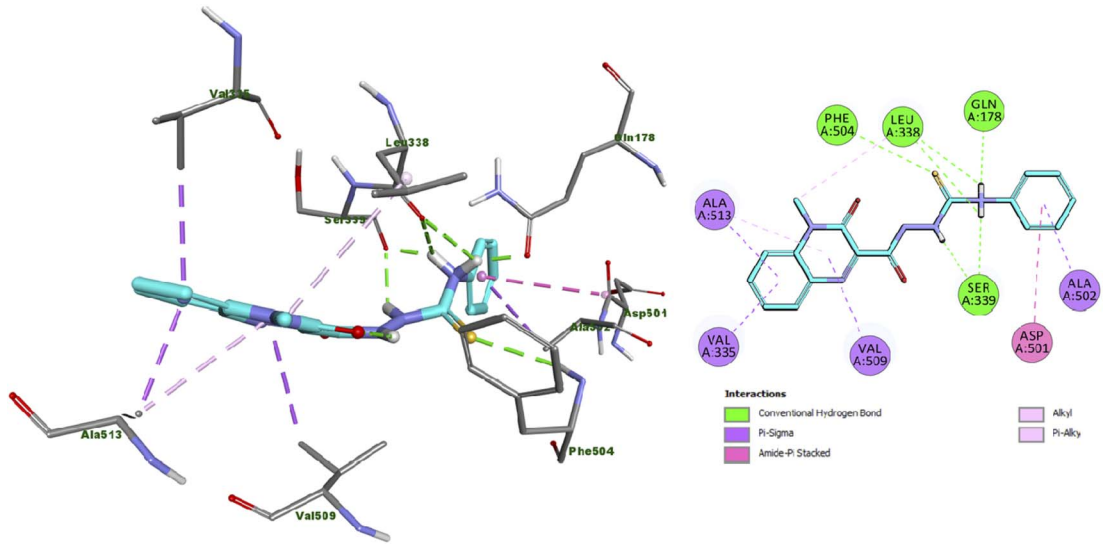

Fig. 2 Docking and binding mode of **13** into the active site of COX2 (PDB ID: 3LN1) (A) 3D structure of **13** (cyan) (B) 2D structure of **13** (cyan).

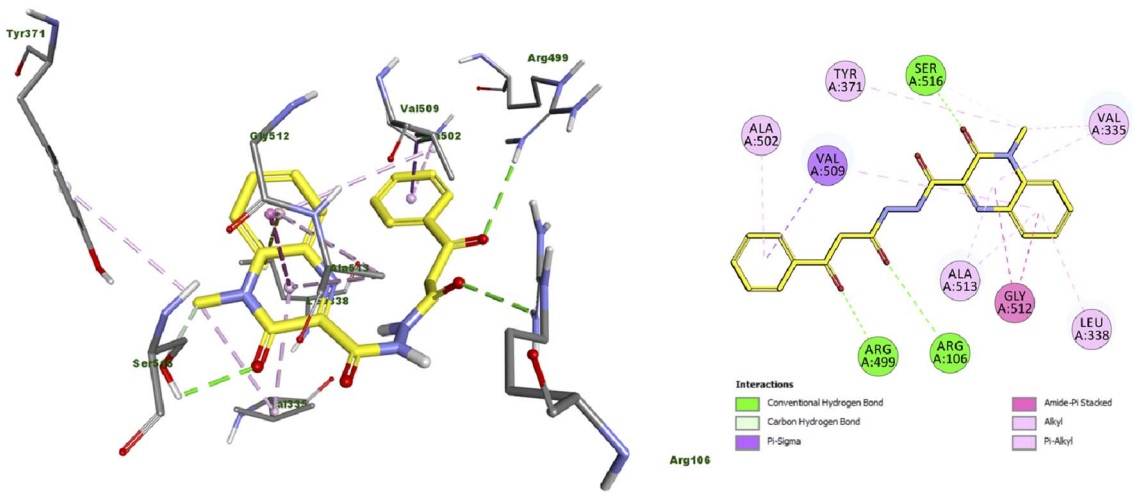

Fig. 3 Docking and binding mode of **11** into the active site of COX2 (PDB ID: 3LN1) (A) 3D structure of **11** (yellow) (B) 2D structure of **11** (yellow).

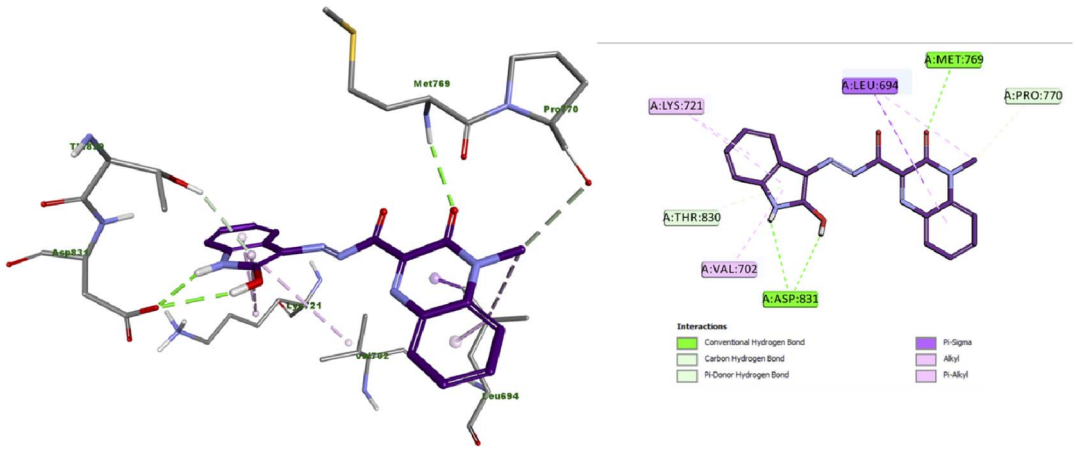

Fig. 4 Docking and binding mode of **4a** into the active site of EGFR (PDB ID: 1M17) (A) 3D structure of **4a** (violet) (B) 2D structure of **4a** (violet).

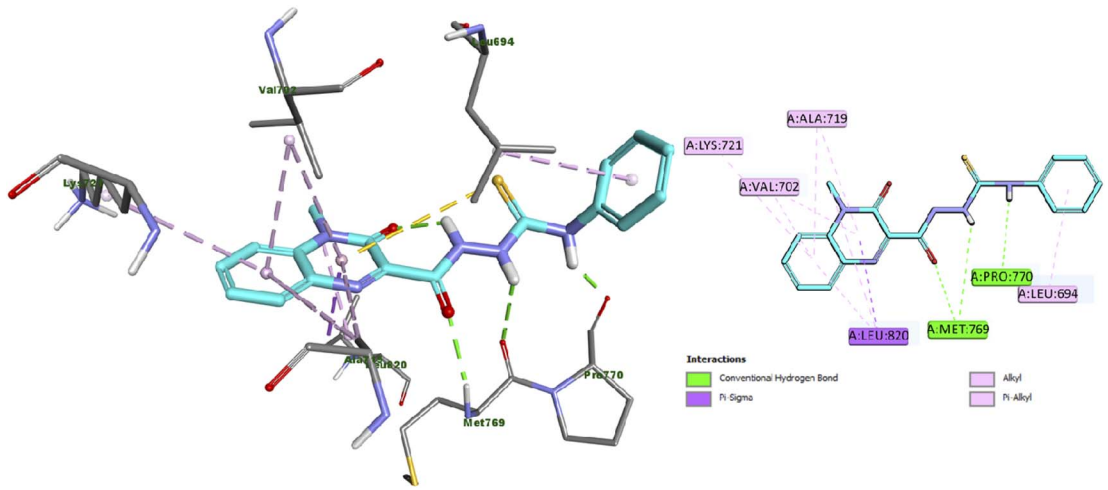

Fig. 5 Docking and binding mode of **13** into the active site of EGFR (PDB ID: 1M17) (A) 3D structure of **13** (cyan) (B) 2D structure of **13** (cyan).

hydrophobic interactions such as Pi-Sigma, amide-pi shaped, alkyl and pi–alkyl interactions with Val335, Asp501, Ala502, Val509 and Ala513 amino acid residues as presented in Fig. 2.

Moreover, the docking results of compound **11** (Fig. 3) showed that it engaged in three hydrogen bonds with Arg106, Arg499 and Ser516 amino acid residues. Additionally, it exhibited many hydrophobic interactions such as carbon hydrogen bond, pi-sigma, amide-pi stacked, alkyl and pi–alkyl interaction with Val335, Leu338, Tyr371, Ala502, Val509, Gly512 and Ala513 amino acid residues.

3.2. Molecular docking study of EGFR (PDB ID: 1M17)

The docking results of compound **4a** (Fig. 4) showed that it formed three hydrogen bonds with Met769 and Asp831 (two HBs). Additionally, compound **4a** presented many hydrophobic interactions such as carbon hydrogen bond, pi-donor hydrogen bond, pi-sigma, alkyl and pi–alkyl interactions with Leu694, Val702, Lys721, Pro770 and Thr830 amino acid residues.

Furthermore, the docking results of compound **13** displayed that it engaged in the formation of three hydrogen bonds with Met769 (two HB) and Pro770 amino acid residues. Also, compound **13** engaged in the formation of numerous hydrophobic interactions as pi-sigma, alkyl and pi–alkyl interactions with Leu694, Val702, Val721, Lys721 and Leu820 amino acid residues as illustrated in Fig. 5.

Collectively, the docking results were in good agreement with the biological screening results suggesting that compounds **4a**, **5**, **11** and **13** are promising dual anticancer candidates *via* inhibition of EGFR-TK enzyme and anti-inflammatory agents *via* inhibition of COX-2 enzyme.

4. Calculations of Lipinski's rule and other *in silico* parameters

Oral bioavailability is a crucial factor in the development of therapeutically bioactive candidates.[45,46] Thus, Lipinski formulated his rule (Rule of Five) for prediction of oral bioavailability as well as drug likeness.[47] This rule depends on using some descriptors as molecular weight, lopP (partition coefficient), hydrogen bond acceptors and donors.[48] Later, Veber added

Table 4 Estimated Lipinski's rule of five and other *in silico* parameters for compounds **4a**, **5**, **11** and **13**

Comp.	MW[c]	Log P[d]	HBA[e]	HBD[f]	nRB[g]	nVs[h]	TPSA[i]	% ABS[j]
Lipinski[a]	≤500	≤5	≤10	≤5	—	≤1	—	—
Veber[b]	—	—	—	—	≤10	—	≤140	—
4a	347.33	1.88	8	2	2	0	109.22	71.13
5	388.38	2.57	8	1	3	0	106.57	72.23
11	364.36	1.18	8	2	5	0	110.16	70.99
13	353.41	1.69	7	3	5	0	88.05	78.62

[a] Reference values of Lipinski. [b] Reference values of Veber. [c] MW, molecular weight. [d] LogP, lipophilicity (O/W). [e] HBA, number of hydrogen bond acceptors. [f] HBD, number of hydrogen bond donors. [g] nRB, number of rotatable bonds. [h] nVs, number of Lipinski rule violations. [i] TPSA, topological polar surface area (PSA) (Å^2). [j] % ABS, percentage of oral absorption.

extra parameters for drug bioavailability such as nRB (number of rotatable bonds) and TPSA (topological polar surface area).[49] Therefore, prediction of Lipinski rule of five and Veber's standards for the most potent quinoxaline derivatives **4a**, **5**, **11** and **13** were performed *via* the Pre-ADMET on line server. As shown in Table 4, all the estimated quinoxaline derivatives have no violation and in full accordance to Lipinski's rule and Veber's standards.

The molecular weight of all predicted quinoxaline derivatives was less than 500, also, they presented LogP values in the range of 1.18 to 2.57 (LogP < 5) and the number of hydrogen bond acceptors and donors in all derivatives were in the acceptable range (HBA < 10 and HBD < 5), which indicated that all estimated quinoxaline derivatives met all criteria of Lipiski's rule of five. Regarding Veber's standards, the number of rotatable bonds were less than 10 and the topological polar surface areas (TPSA) were found in the range of 88.05 to 110.16 Å^2 (<140 Å^2), which accorded to Veber's rule. The percentage of oral absorption (% ABS) values of all estimated quinoxaline derivatives ranged from 70.99% to 78.62%, indicating that these derivatives would have acceptable molecular flexibilities and accordingly good membrane permeability and good oral bioavailability. Based on these results, we could conclude that hybrids **4a**, **5**, **11** and **13** can be served as good orally-absorbed dual acting antitumor and anti-inflammatory candidates and these properties can be improved by further modifications and SAR studies.

5. Structure activity relationship

Study of the structure activity relationship (SAR), as illustrated in Fig. 6, showed that, presence of hydrazone or hydrazide group is essential for both anticancer and COX-2 inhibitory activities. Moreover, polar hyrazones or polar groups are not favored and results in decrease or abolishment of the anticancer or COX-2 inhibitory activities. Additionally, the presence of oxygen at position 2 is essential for activity if it is replaced with other group, as in compound **10**, results in significant decrease in both the potency and broadness. Ongoing throughout the results, it is obvious that the hydrazide obtained from the reaction of compound **1** with ethylacetoacetate (**8**), benzoylacetone (**9**), showed high activity; when R^1 = phenyl and R^2 = methyl (**9**) > R^1 = methyl and R^2 = ethoxy (**8**). Also, introducing the coumarin moiety, significantly improved both the anticancer and COX-2 inhibitory activities (**5**). Shifting to isatin (**4a**) enhanced the activity as anticancer and COX-2 inhibitor, while replacement with *N*-methyl isatin (**4b**) resulted in decrease in the anticancer activity. *N*-benzylidene derivatives(**2a–d**)are still

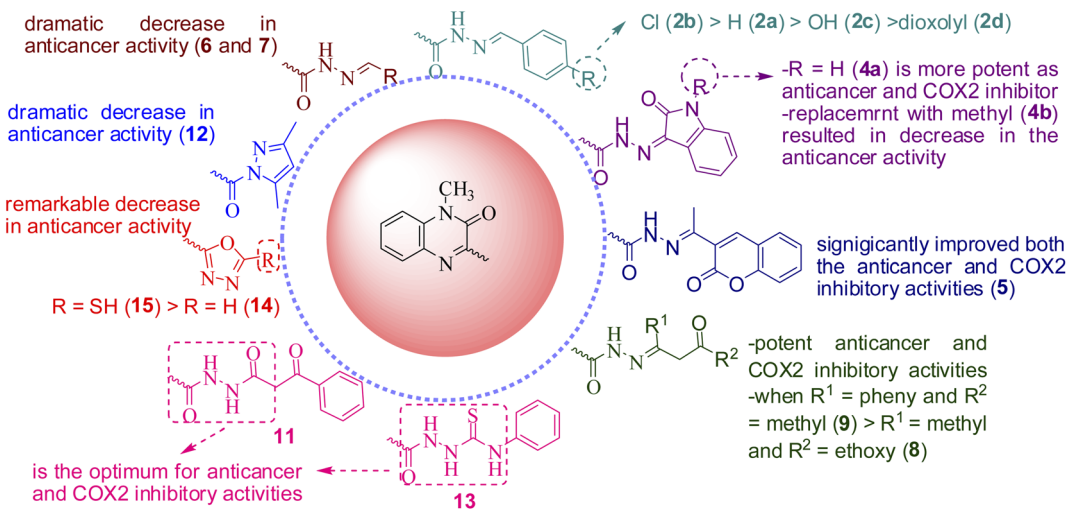

Fig. 6 Structure activity relationship (SAR) for the newly synthesized quinoxaline derivatives.

active, in particular, inpresence of lipophilic electron withdrawing group as Cl (**2b**) is the most potent while substitution with polar donating groups such as OH or dioxolyl group (**2c** and **2d**, respectively) led to significant decrease in the activity. The order of activity is as follows; Cl > H > OH > dioxolyl. On contrary, hydrazides obtained from polar aldehydes such as arabinose or glucoseled to a dramatic decrease in anticancer activity. Additionally, masking the hydrazide group *via* incorporation of five membered rings remarkably decreased the anticancer activity (**12**, **14** and **15**). Finally, substitution with ethyl benzoyl acetate (**11**), phenyl isothiocyanate (**13**), seems to be the optimum for anticancer and COX-2 inhibitory activities.

6. Conclusion

In summary, 18 novel quinoxaline derivatives have been synthesized and evaluated for their anticancer and COX inhibitory activities. Most of the tested compounds displayed good anticancer and COX-2 inhibitory activities. In particular, quinoxaline derivatives **11** and **13** exhibited potent anticancer activity against the three cancer cell lines with IC_{50} values ranging from 0.81 μM to 2.91 μM. Also, compounds **4a** and **5** showed strong anticancer activity against the three-cancer cell line with IC_{50} values ranging from 3.21 μM to 4.54 μM. These derivatives strongly inhibited EGFR with IC_{50} values in the range of 0.3–0.9 μM. Regarding COX enzyme inhibition, compounds **4a**, **5**, **11** and **13** were more potent and selective against COX-2 than COX-1, among them, compounds **11** and **13** were the most potent as COX-2 inhibitors and showed higher potency against COX-2 (IC_{50} = 0.62 and 0.46 μM, respectively) more than COX-1 (IC_{50} = 37.96 and 30.41 μM, respectively) with selectivity indexes (SI) of 61.23 and 66.11, respectively. Compound **5** comes next with IC_{50} = 0.83 μM and SI of 48.58. Finally, compounds **4a** were the least active with IC_{50} values equal to 1.17 μM and SI of 24.61. The molecular docking into the catalytic binding pocket of the both protein receptors; EGFR (PDB ID: 1M17) and COX-2 (PDB ID: 3LN1) strongly correlated with the biological results. The calculated parameters of Lipinski's rule of five were and Veber's standards revealed that compounds **4a**, **5**, **11** and **13** had a reasonable drug-likeness with acceptable physicochemical properties. Based on the obtained results of biological investigation as well as molecular docking study and physiochemical parameters, it could be concluded that quinoxalinehydrazide derivatives, particularly, **4a**, **5**, **11** and **13** are promising scaffold for innovation and discovery of new bioactive candidates. Moreover, compounds **4a**, **5**, **11** and **13** might be used as promising orally absorbed dual anticancer candidates *via* inhibition of EGFR enzyme and anti-inflammatory agents *via* inhibition of COX-2 enzyme and entitled to be used as a future template for further modifications and more SAR study.

7. Experimental

7.1. Chemistry

For details; see ESI File.†

7.1.1 General procedure for the synthesis of *N′*-arylidene-4-methyl-3-oxo-3,4-dihydroquinoxaline-2-carbohydrazide (2a–d and 3) (4a, 4b). A mixture of compound **1** (0.218 g, 0.001 mol) and the appropriate aromatic aldehyde or isatins (0.001 mol) was stirred under reflux in absolute ethanol (10 mL) for 2 hours. The solid product was precipitated on hot, collected by filtration, washed with ethanol and recrystallized from dimethyl formamide DMF.

7.1.2 *N′*-benzylidene-4-methyl-3-oxo-3,4-dihydroquinoxaline-2-carbohydrazide (2a). White crystals. Mp. 260–262 °C, yield (0.254 g, 83%). IR (KBr) *ν*: 3173 (NH), 3070 (CH-aromatic), 2973, 2866 (CH-aliphatic), 1674 (C=O), 1640 (C=O) cm^{-1}; ^{1}H NMR (DMSO-d_6) *δ*: 12.47 (s, 1H, NH disappeared on addition of D_2O), 8.35 (s, 1H, $=CH_{Schiffbase}$), 8.02–7.58 (m, 3H, $H_{arom.}$), 7.57–7.18 (m, 6H, $H_{arom.}$), 3.74 (s, 3H, N–CH_3). ^{13}C NMR (DMSO-d_6) *δ*: 166.9, 159.4, 154.5, 154.0, 152.5, 149.9, 147.9, 145.3, 134.1, 133.9, 133.9, 133.7, 133.0, 132.3, 132.1, 131.5, 131.1, 130.6, 130.1, 128.8, 128.7, 127.8, 127.0, 124.6, 124.0, 114.9, 114.8, 29.6, 29.1. Anal. calcd for $C_{17}H_{14}N_4O_2$ (306.32): C, 66.66; H, 4.61; N, 18.29; O, 10.45, found: C, 66.62; H, 4.65; N, 18.33.

7.1.3 (*E*)-*N′*-(4-chlorobenzylidene)-4-methyl-3-oxo-3,4-dihydroquinoxaline-2-carbohydrazide (2b). Yellowish white crystals. Mp. 258–260 °C, yield (0.31 g, 91%). IR (KBr) *ν*: 3165 (NH), 3074 (CH-aromatic), 2919, 2848 (CH-aliphatic), 1706 (C=O) cm^{-1}; ^{1}H NMR (DMSO-d_6) *δ*: 12.27 (s, 1H, NH disappeared on addition of D_2O), 8.06 (s, 1H, $=CH_{Schiffbase}$), 7.98–7.68 (dd, 1H, $H_{arom.}$), 7.83–7.63 (m, 3H, $H_{arom.}$), 7.58–7.54 (d, 1H, $H_{arom.}$), 7.53–7.43 (m, 1H, $H_{arom.}$), 7.39 (s, 2H, $H_{arom.}$),3.71 (s, 3H, N–CH_3). ^{13}C NMR (DMSO-d_6) *δ*: 166.9, 160.3, 154.5, 153.3, 152.5, 150.6, 148.0, 144.2, 135.3, 134.9, 134.2, 133.8, 133.3, 132.9, 132.8, 132.0, 132.0, 131.9, 130.5, 130.1, 129.4, 129.4, 129.4, 128.7, 124.6, 124.4, 115.7, 115.6, 29.6, 29.4. Anal. calcd for $C_{17}H_{13}ClN_4O_2$ (340.76): C, 59.92; H, 3.85; Cl, 10.40; N, 16.44. Found: C, 59.88; H, 3.82; Cl, 10.43; N, 16.47.

7.1.4 *N′*-(4-hydroxybenzylidene)-4-methyl-3-oxo-3,4-dihydroquinoxaline-2-carbohydrazide (2c). Yellow crystals. Mp. 318–320 °C, yield (0.28 g, 87%). IR (KBr) *ν*: 3215 (OH), 3148 (NH), 3055 (CH-aromatic), 2919 (CH-aliphatic), 1672 (C=O) cm^{-1}; ^{1}H NMR (DMSO-d_6) *δ*: 12.03 (s, 1H, NH disappeared on addition of D_2O), 10.09–9.87 (d, 1H, OH), 7.96–7.94 (m, 1H, $H_{arom.}$), 7.90–7.88 (d, 1H,=CH $_{Schiffbase}$), 7.80–7.70 (m, 2H, $H_{arom.}$), 7.68–7.58 (d, 1H, $H_{arom.}$), 7.54–7.46 (m, 1H, $H_{arom.}$), 7.22–7.16 (d, 1H, $H_{arom.}$), 6.90–6.85 (d, 1H, $H_{arom.}$), 6.73–6.69 (d, 1H, $H_{arom.}$), 3.71 (s, 3H, N–CH_3). ^{13}C NMR (DMSO-d_6) *δ*: 166.5, 160.2, 159.9, 159.7, 154.8, 153.4, 152.5, 150.7, 149.6, 145.7, 134.1, 133.8, 132.8, 132.0, 131.9, 131.9, 130.5, 130.0, 129.7, 128.9, 125.3, 125.0, 124.6, 124.4, 116.2, 116.1, 115.6, 115.6, 29.6, 29.4. Anal. calcd for $C_{17}H_{14}N_4O_3$ (322.32): C, 63.35; H, 4.38; N, 17.38. Found: C, 63.35; H, 4.38; N, 17.38.

7.1.5 (*E*)-*N′*-(benzo[*d*][1,3]dioxol-5-ylmethylene)-4-methyl-3-oxo-3,4-dihydroquinoxaline-2-carbohydrazide (2d). Yellow crystals. Mp. 284–285 °C, yield (0.31 g, 86%). IR (KBr) *ν*: 3148 (NH), 3074 (CH-aromatic), 2977, 2880 (CH-aliphatic), 1682 (C=O) cm^{-1}; ^{1}H NMR (DMSO-d_6) *δ*: 12.10 (s, 1H, NH disappeared on addition of D_2O), 8.25–6.85 (m, 8H, =CH + $H_{arom.}$), 6.00 (s, 2H,

CH_2), 3.69 (s, 3H, N–CH_3). Anal. calcd for $C_{18}H_{14}N_4O_4$ (350.33): C, 61.71; H, 4.03; N, 15.99. Found: C, 61.75; H, 3.99; N, 15.96.

7.1.6 (*N*′,*N*″*E*,*N*′,*N*″*E*)-*N*′,*N*″-(1,2-phenylenebis(methan-1-yl-1-ylidene))bis(4-methyl-3-oxo-3,4-dihydroquinoxaline-2-carbohydrazide) (3). Yellow crystals. Mp. 242–243 °C, yield (0.28 g, 85%). IR (KBr) *ν*: 3197 (NH), 3132 (NH), 3052 (CH-aromatic), 2979, (CH-aliphatic), 1690 (C=O), 1660 (C=O) cm^{-1}; ^1H NMR (DMSO-d_6) *δ*: 12.43–12.18 (dd, 2H, 2NH disappeared on addition of D_2O), 8.86–7.28 (m, 14H, =CH + $H_{arom.}$), 3.71 (s, 6H, 2N–CH_3). Anal. calcd for $C_{18}H_{14}N_4O_3$ (334.33): C, 64.66; H, 4.22; N, 16.76. Found: C, 64.62; H, 4.19; N, 16.81.

7.1.7 (*Z*)-4-Methyl-3-oxo-*N*′-(2-oxoindolin-3-ylidene)-3,4-dihydroquinoxaline-2-carbohydrazide (4a). Orange crystals. Mp. > 330 °C, yield (0.29 g, 86%). IR (KBr) *ν*: 3197 (NH), 3132 (NH), 3058 (CH-aromatic), 2885, (CH-aliphatic), 1705 (C=O) cm^{-1}; ^1H NMR (DMSO-d_6) *δ*: 13.21 (s, 1H, NH disappeared on addition of D_2O), 10.93 (s, 1H, NH disappeared on addition of D_2O), 8.26–8.19 (d, 1H, $H_{arom.}$), 8.12–8.08 (d, 1H, $H_{arom.}$), 7.92–7.87 (t, 1H, $H_{arom.}$), 7.82–7.78 (d, 1H, $H_{arom.}$), 7.62–7.56 (t, 1H, $H_{arom.}$), 7.51–7.45 (t, 1H, $H_{arom.}$), 7.21–7.16 (t, 1H, $H_{arom.}$), 7.00–6.96 (d, 1H, $H_{arom.}$), 3.83 (s, 3H, N–CH_3). ^{13}C NMR (DMSO-d_6) *δ*: 166, 160, 159, 155, 144, 143, 134.1, 133.8, 131.5, 125.3, 125.1, 123.0, 122.6, 115.9, 115.7, 115.5, 111.6, 30.3. Anal. calcd for $C_{18}H_{13}N_5O_3$ (347.33): C, 62.24; H, 3.77; N, 20.16. Found: C, 62.21; H, 3.81; N, 20.13.

7.1.8 (*Z*)-4-Methyl-*N*′-(1-methyl-2-oxoindolin-3-ylidene)-3-oxo-3,4-dihydroquinoxaline-2-carbohydrazide (4b). Orange crystals, mp. 325–326 °C, yield (0.28 g, 78%). IR (KBr) *ν*: 3197 (NH), 3051 (CH-aromatic), 2927, 2881, (CH-aliphatic), 1702 (C=O) cm^{-1}; ^1H NMR (DMSO-d_6) *δ*: 13.26 (s, 1H, NH disappeared on addition of D_2O), 8.28–7.15 (m, 8H, $H_{arom.}$), 3.83 (s, 3H, N–CH_3), 3.24 (s, 3H, N–CH_3). Anal. calcd for $C_{19}H_{15}N_5O_3$ (361.35): C, 63.15; H, 4.18; N, 19.38. Found: C, 63.11; H, 4.21; N, 19.41.

7.1.9 (*E*)-4-Methyl-3-oxo-*N*′-(1-(2-oxo-2*H*-chromen-3-yl) ethylidene)-3,4-dihydroquinoxaline-2-carbohydrazide (5). A mixture of **1** (0.218 g, 0.001 mol), acetyl coumarin (0.188 g, 0.001 mol) in dioxane (20 mL) was refluxed for 3 h. The solid product was precipitated on hot, collected by filtration, dried and recrystallized from DMF to give pale yellow crystals. Mp. 305–306 °C, yield (0.27 g, 71%). IR (KBr) *ν*: 3179 (NH), 3089 (CH-aromatic), 2988 (CH-aliphatic), 1727 and 1655 (2C=O) cm^{-1}; ^1H NMR (DMSO-d_6) *δ*: 12.01 (s, 1H, NH disappeared on addition of D_2O), 8.34–7.29 (m, 9H, =CH + $H_{arom.}$), 3.75 (s, 3H, N–CH_3 quinoxaline), 2.29 (s, 3H, CH_3). Anal. calcd for $C_{21}H_{16}N_4O_4$ (388.38): C, 64.94; H, 4.15; N, 14.43. Found: C, 64.91; H, 4.18; N, 14.47.

7.1.10 (*E*)-4-Methyl-3-oxo-*N*′-(2,3,4,5-tetrahydroxypentylidene)-3,4-dihydroquinoxaline-2-carbohydrazide (6). A mixture of **1** (0.218 g, 0.001 mol), arabinose (0.15 g, 0.001 mol) in absolute ethanol (20 mL) was refluxed for 3 h. After cooling, the solid product was collected by filtration and recrystallized from ethanol to give white crystals. Mp. 210–211 °C, yield (0.22 g, 64%). IR (KBr) *ν*: 3456 (OH), 3395 (OH), 3338 (OH), 3303 (OH), 3176 (NH), 3034 (CH-aromatic), 2973, 2868 (CH-aliphatic), 1678 (C=O) cm^{-1}; ^1H NMR (DMSO-d_6) *δ*: 10.41 (s, 1H, NH exchanged with D_2O), 7.96–7.92 (d, 1H, $H_{arom.}$), 7.80–7.74 (t, 1H, $H_{arom.}$), 7.70–7.65 (d, 1H, $H_{arom.}$), 7.51–7.45 (t, 1H, $H_{arom.}$), 6.15–6.10 (t, 1H, OH), 6.08–6.04 (d, 1H, =CH), 5.04–5.03 (d, 1H, OH), 4.96–4.93 (d, 1H, OH), 4.57–4.56 (d, 1H, OH), 4.46–4.43 (d, 1H, CH), 3.96–3.91 (t, 1H, CH), 3.80–3.76 (d, 1H, CH), 3.69 (s, 3H, NCH_3), 3.55–3.49 (m, 2H, CH_2); ^{13}C NMR (DMSO-d_6) *δ*: 166.6, 162.2, 155.3, 153.6, 149.9, 134.0, 132.6, 131.8, 130.6, 124.5, 115.6, 93.2, 91.3, 69.7, 68.0, 67.8, 63.1, 29.6. Anal. calcd for $C_{15}H_{18}N_4O_6$ (350.33): C, 51.43; H, 5.18; N, 15.99. Found: C, 51.39; H, 5.21; N, 16.02.

7.1.11 (*E*)-4-Methyl-3-oxo-*N*′-(2,3,4,5,6-pentahydroxyhexylidene)-3,4-dihydroquinoxaline-2-carbohydrazide (7). A mixture of **1** (0.218 g, 0.001 mol), glucose (0.18 g, 0.001 mol) in absolute ethanol (20 mL) was refluxed for 3 h. The solid product was precipitated on hot, collected by filtration, washed with ice ethanolic solution, dried and recrystallized from ethanol to give white crystals. Mp. 170–171 °C, yield (0.31 g, 82%).

IR (KBr) *ν*: 3570 (OH), 3441 (OH), 3388 (OH), 3366 (OH), 3258 (OH), 3169 (NH), 3070 (CH-aromatic), 2918, 2850 (CH-aliphatic), 1704 (C=O), 1649 (C=O) cm^{-1}; ^1H NMR (DMSO-d_6) *δ*: 10.33 (s, 1H, NH exchanged with D_2O), 7.93–7.91 (d, 1H, $H_{arom.}$), 7.81–7.74 (t, 1H, $H_{arom.}$), 7.69–7.58 (d, 1H, $H_{arom.}$), 7.50–7.40 (t, 1H, $H_{arom.}$), 6.09–6.05 (t, 1H, OH), 5.63–5.59 (d, 1H, =CH), 5.11–5.08 (t, 1H, OH), 5.02–4.98 (d, 1H, OH), 4.95–4.92 (d, 1H, OH), 4.45–4.43 (t, 1H, OH), 3.92–3.88 (dd, 1H, CH), 3.68 (s, 3H, NCH_3), 3.51–2.84 (m, 5H, H_{aliph}). Anal. calcd for $C_{16}H_{20}N_4O_7$ (380.35): C, 50.52; H, 5.30; N, 14.73. Found: C, 50.48; H, 5.35; N, 14.77.

7.1.12 (*E*)-Ethyl 3-(2-(4-methyl-3-oxo-3,4-dihydroquinoxaline-2-carbonyl)hydrazono) butanoate (8). A mixture of **1** (0.218 g, 0.001 mol), ethylacetoacetate (0.13 g, 0.001 mol) in absolute ethanol (20 mL) was refluxed for 5 h. After cooling, the solid product was collected by filtration and recrystallized from ethanol to give white crystals. Mp. 218–219 °C, yield (0.26 g, 81%). IR (KBr) *ν*: 3168 (NH), 3095 (CH-aromatic), 2982, 2921 (CH-aliphatic), 1703 (C=O), 1631 (C=O) cm^{-1}; ^1H NMR (DMSO-d_6) *δ*: 11.06 (s, 1H, NH disappeared on addition of D_2O), 7.99–7.95 (d, 1H, $H_{arom.}$), 7.83–7.77 (t, 1H, $H_{arom.}$), 7.54–7.48 (t, 1H, $H_{arom.}$), 4.16–4.11 (q, 2H, CH_2), 3.72 (s, 3H, N–CH_3), 3.46 (s, 2H, CH_2CO), 1.99 (s, 3H, CH_3C=N), 1.27–1.22 (t, 3H, CH_3CH_2). ^{13}C NMR (DMSO-d_6) *δ*: 169.9, 169.2, 167.5, 159.7, 155.2, 154.2, 153.2, 152.3, 149.7, 149.3, 134.1, 134.0, 133.7, 132.9, 132.3, 131.9, 131.7, 130.7, 129.9, 124.7, 124.2, 115.6, 115.5, 61.0, 60.4, 44.3, 44.2, 29.8, 29.3, 17.2, 17.0, 14.5, 14.4, 14.1. Anal. calcd for $C_{16}H_{18}N_4O_4$ (330.34): C, 58.17; H, 5.49; N, 16.96. Found: C, 58.21; H, 5.53; N, 17.01.

7.1.13 Benzoylacetone: (*Z*)-4-methyl-3-oxo-*N*′-(3-oxo-1-phenylbutylidene)-3,4-dihydroquinoxaline-2-carbohydrazide (9). A mixture of **1** (0.218 g, 0.001 mol), benzoylacetone (0.16 g, 0.001 mol) in absolute ethanol (20 mL) was refluxed for 5 h. After cooling, the solid product was collected by filtration and recrystallized from ethanol to give orange crystals. Orange crystals. Mp. 219–220 °C, yield (0.28 g, 77.7%). IR (KBr) *ν*: 3152 (NH), 3067 (CH-aromatic), 2956, 2916 (CH-aliphatic), 1689 (C=O), 1626 (C=O) cm^{-1}; ^1H NMR (DMSO-d_6) *δ*: 12.73 (s, 1H, NH exchanged with D_2O), 11.43 (s, 1H, OH exchanged with D_2O), 8.00–7.96 (d, 1H, $H_{arom.}$), 7.95–7.91 (d, 1H, $H_{arom.}$), 7.84–7.79 (t,

1H, $H_{arom.}$), 7.74–7.70 (d, 1H, $H_{arom.}$), 7.63–7.56 (t, 1H, $H_{arom.}$), 7.54–7.46 (t, 3H, $H_{arom.}$), 7.44–7.39 (t, 1H, $H_{arom.}$), 6.07 (s, 1H, =CH), 3.73 (s, 3H, NCH_3), 2.18 (s, 3H, CH_3). Anal. calcd for $C_{20}H_{18}N_4O_3$ (362.38): C, 66.29; H, 5.01; N, 15.46. Found: C, 66.33; H, 4.97; N, 15.49.

7.1.14 3-Diazenyl-4-methyl-3,4-dihydroquinoxaline-2-carbohydrazide (10). A mixture of **1** (0.218 g, 0.001 mol), hydrazine hydrate (0.06 g, 0.0012 mol) in absolute ethanol (20 mL) was refluxed for 2 h. The solid product was precipitated on hot, collected by filtration, dried and recrystallized from ethanol to give white crystals. Mp. 220–221 °C, yield (0.17 g, 74%). IR (KBr) ν: 3350, 3312, 3215 (NH_2 + 2NH), 3051 (CH-aromatic), 2920, 2862 (CH-aliphatic), 1645 (C=O) cm^{-1}; ^1H NMR (DMSO-d_6) δ: 9.42 (s, 1H, NH disappeared on addition of D_2O), 7.25–6.96 (dd, 2H, $H_{arom.}$), 6.82–6.77 (t, 1H, $H_{arom.}$), 6.70–6.66 (d, 1H, $H_{arom.}$), 4.43 (s, 1H, CH), 4.34 (s, 2H, NH_2 disappeared on addition of D_2O), 3.39 (s, 1H, NH disappeared on addition of D_2O), 2.79 (s, 3H, N–CH_3). ^{13}C NMR (DMSO-d_6) δ: 166.0, 163.8, 136.6, 135.1, 129.0, 123.6, 118.4, 114.5, 111.2, 66.0, 35.5, 29.0. Anal. calcd for $C_{10}H_{12}N_6O$ (232.24): C, 51.72; H, 5.21; N, 36.19. Found: C, 51.68; H, 5.24; N, 36.23.

7.1.15 4-Methyl-3-oxo-*N*′-(3-oxo-3-phenylpropanoyl)-3,4-dihydroquinoxaline-2-carbohydrazide (11). A mixture of **1** (0.218 g, 0.001 mol), ethyl benzoyl acetate (0.192 g, 0.001 mol) in dioxane (20 mL) was refluxed for 8 h. After cooling, the solid product was collected by filtration and recrystallized from dioxane to give orange crystals. Mp. 230–231 °C, yield (0.23 g, 65%). IR (KBr) ν: 3159 (NH), 3059 (CH-aromatic), 2917, 2848 (CH-aliphatic), 1681 (C=O), 1633 (C=O) cm^{-1}; ^1H NMR (DMSO-d_6) δ: 11.39 (s, 1H, NH disappeared on addition of D_2O), 11.05 (s, 1H, NH disappeared on addition of D_2O), 8.06–7.47 (m, 9H, $H_{arom.}$), 4.1 (s, 2H, CH_2), 3.70 (s, 3H, N–CH_3). ^{13}C NMR (DMSO-d_6) δ: 194.5, 169.9, 168.9, 164.3, 160.3, 153.6, 148.9, 136.5, 134.1, 133.0, 132.0, 130.7, 129.3, 129.2, 128.9, 125.8, 124.7, 115.7, 45.3, 29.7. Anal. calcd for $C_{19}H_{16}N_4O_4$ (364.35): C, 62.63; H, 4.43; N, 15.38. Found: C, 62.66; H, 4.39; N, 15.42.

7.1.16 3-(3,5-Dimethyl-1*H*-pyrazole-1-carbonyl)-1-methylquinoxalin-2(1*H*)-one (12). A mixture of **1** (0.218 g, 0.001 mol), acetylacetone (0.100 g, 0.001 mol) in absolute ethanol (20 mL) was refluxed for 5 h. After cooling, the solid product was collected by filtration and recrystallized from ethanol to give white crystals. Mp. 265–266 °C, yield (0.24 g, 85%). IR (KBr) ν: 3045 (CH-aromatic), 2979, 2865 (CH-aliphatic), 1721 (C=O), 1648 (C=O) cm^{-1}; ^1H NMR ($CDCl_3$) δ: 7.99–7.94 (d, 1H, $H_{arom.}$), 7.68–7.64 (t, 1H, $H_{arom.}$), 7.46–7.40 (t, 1H, $H_{arom.}$), 7.30 (s, 1H, $H_{arom.}$), 6.07 (s, 1H, $H_{pyrazole}$), 3.77 (s, 3H, N–CH_3), 2.72 (s, 3H, CH_3), 2.16 (s, 3H, CH_3). ^{13}C NMR ($CDCl_3$) δ: 159.6, 149.5, 148.3, 148.1, 139.6, 129.1, 127.6, 126.9, 126.2, 119.3, 109.2, 107.2, 24.3, 9.2, 9.1. Anal. calcd for $C_{15}H_{14}N_4O_2$ (282.30): C, 63.82; H, 5.00; N, 19.85. Found: C, 63.86; H, 4.96; N, 19.89.

7.1.17 2-(4-Methyl-3-oxo-3,4-dihydroquinoxaline-2-carbonyl)-*N*-phenylhydrazine-carbothioamide (13). A mixture of **1** (0.218 g, 0.001 mol), phenyl isothiocyanate (0.135 g, 0.001 mol) in absolute ethanol (20 mL) was refluxed for 1 h. The solid product was precipitated on hot, collected by filtration, dried and recrystallized from DMF to give yellow crystals. Mp. 261–263 °C, yield (0.31 g, 90%). IR (KBr) ν: 3253 (NH), 3204 (NH), 3145 (NH), 3089 (CH-aromatic), 2979, 2941 (CH-aliphatic), 1661 (C=O), 1631 (C=O) cm^{-1}. ^1H NMR (DMSO-d_6) δ: 11.02 (br, 1H, NH disappeared on addition of D_2O), 10.20 (br, 1H, NH disappeared on addition of D_2O), 9.81 (br, 1H, NH disappeared on addition of D_2O), 8.00–7.98 (d, 1H, $H_{arom.}$), 7.85–7.81 (t, 1H, $H_{arom.}$), 7.77–7.73 (d, 1H, $H_{arom.}$), 7.67–7.63 (d, 2H, $H_{arom.}$), 7.58–7.52 (t, 1H, $H_{arom.}$), 7.42–7.36 (t, 2H, $H_{arom.}$), 7.23–7.17 (t, 1H, $H_{arom.}$), 3.76 (s, 3H, N–CH_3). ^{13}C NMR (DMSO-d_6) δ: 154.3, 139.3, 133.9, 133.2, 132.3, 130.8, 128.8, 125.0, 115.9, 30.0. Anal. calcd for $C_{17}H_{15}N_5O_2S$ (353.40): C, 57.78; H, 4.28; N, 19.82; S, 9.07. Found: C, 57.82; H, 4.24; N, 19.78; S, 9.12.

7.1.18 1-Methyl-3-(1,3,4-oxadiazol-2-yl)quinoxalin-2(1*H*)-one (14). A mixture of **1** (0.218 g, 0.001 mol) and triethylorthoformate (5 mL) was refluxed for 11 h. After cooling, the solid product was collected by filtration and recrystallized from DMF to give yellow crystals. Mp. 225–226 °C, yield (0.14 g, 65%). IR (KBr) ν: 3052 (CH-aromatic), 2915, 2848 (CH-aliphatic), 1643 (C=O) cm^{-1}. ^1H NMR (DMSO-d_6) δ: 9.52 (s, 1H, $H_{oxadiazole}$), 7.99–7.41 (m, 4H, $H_{arom.}$), 3.72 (s, 3H, N–CH_3). ^{13}C NMR (DMSO-d_6) δ: 161.0, 155.5, 152.4, 141.3, 134.7, 133.7, 132.2, 131.0, 124.6, 115.7, 29.9. Anal. calcd for $C_{11}H_8N_4O_2$ (228.21): C, 57.89; H, 3.53; N, 24.55. Found: C, 57.93; H, 3.50; N, 24.51.

7.1.19 1-Methyl-3-(5-thioxo-4,5-dihydro-1,3,4-oxadiazol-2-yl)quinoxalin-2(1*H*)-one (15). A mixture of **1** (0.218 g, 0.001 mol), excess of carbon disulphide (0.3 g, 0.004 mol) in dry pyridine (20 mL) was refluxed for 8 h. The solid product was precipitated on hot, collected by filtration, dried and recrystallized from ethanol to give yellow crystals. Mp. 230–231 °C, yield (0.23 g, 90%).

IR (KBr) ν: 3233 (NH), 3046 (CH-aromatic), 2917, 2847 (CH-aliphatic), 1645 (C=O) cm^{-1}. ^1H NMR (DMSO-d_6) δ: 14.98 (br, 1H, NH disappeared on addition of D_2O), 7.99–7.97 (d, 1H, $H_{arom.}$), 7.82–7.77 (t, 1H, $H_{arom.}$), 7.68–7.66 (d, 1H, $H_{arom.}$), 7.52–7.47 (t, 1H, $H_{arom.}$), 3.70 (s, 3H, N–CH_3). ^{13}C NMR (DMSO-d_6) δ: 157.4, 151.7, 139.1, 134.5, 133.7, 132.1, 130.9, 124.7, 115.6, 29.8. Anal. calcd for $C_{11}H_8N_4O_2S$ (260.27): C, 50.76; H, 3.10; N, 21.53; O, 12.29; S, 12.32. Found: C, 50.80; H, 3.14; N, 21.49; S, 12.33.

7.2. Biological evaluation

7.2.1. Assay for anticancer effect. To explore the anticancer potential of compounds, MTT assay was performed[43] using different cell lines. See ESI File.†

7.2.2. *In vitro* cyclooxygenase (COX) inhibition assay. The *in vitro* cyclooxygenase inhibition assay was performed using the colorimetric COX-1/COX-2 inhibition assay kit (kit catalogue number 560101, Cayman Chemical, Ann Arbour, MI) following the manufacturer's instructions.[50,51] See ESI File.†

7.2.3. EGFR inhibitory assay. A cell-free assay was used to explore the mechanism of inhibition of EGFR kinase of the most active compounds according to the reported method.[43,44] See ESI File.†

8. Docking methodology

For docking analysis, Discovery Studio 2.5 software (Accelrys Inc., San Diego, CA, USA) was used. Fully automated docking tool using "Dock ligands (CDOCKER)" protocol running on

Intel (R) core (TM) i32370 CPU@2.4 GHz 2.4 GHz, RAM Memory 2 GB under the Windows 7.0 system. The 3.5 ÅA 3D crystal structures of EGFR (PDB ID: 1M17)[43,44] and COX-2 (PDB ID: 3LN1)[20,42] were retrieved from protein data bank. See ESI File.†

9. *In silico* prediction of physicochemical properties and pharmacokinetic profile

For prediction of Lipinski's rule (rule of five), molecular property prediction and pre-ADMET estimation; the free accesses to websites **https://www.molsoft.com/servers.html** and **https://preadmet.bmdrc.kr/** were used.

Conflicts of interest

There are no conflicts to declare.

References

1 M. F. Mohamed and G. E.-D. A. Abuo-Rahma, *RSC Adv.*, 2020, **10**, 31139–31155.
2 K. El-Adl, H. M. Sakr, R. G. Yousef, A. B. M. Mehany, A. M. Metwaly, M. A. Elhendawy, M. M. Radwan, M. A. ElSohly, H. S. Abulkhair and I. H. Eissa, *Bioorg. Chem.*, 2021, **114**, 105105.
3 F. A. Rodrigues, S. Bomfim Ida, B. C. Cavalcanti, Ó. Pessoa Cdo, J. L. Wardell, S. M. Wardell, A. C. Pinheiro, C. R. Kaiser, T. C. Nogueira, J. N. Low, L. R. Gomes and M. V. de Souza, *Bioorg. Med. Chem. Lett.*, 2014, **24**, 934–939.
4 A. K. A. Bass, E.-S. M. Nageeb, M. S. El-Zoghbi, M. F. A. Mohamed, M. Badr and G. E.-D. A. Abuo-Rahma, *Bioorg. Chem.*, 2022, **119**, 105564.
5 A. K. A. Bass, M. S. El-Zoghbi, E.-S. M. Nageeb, M. F. A. Mohamed, M. Badr and G. E.-D. A. Abuo-Rahma, *Eur. J. Med. Chem.*, 2021, **209**, 112904.
6 I. Piotrowski, K. Kulcenty and W. Suchorska, *Rep. Pract. Oncol. Radiother.*, 2020, **25**, 422.
7 F. R. Greten and S. I. Grivennikov, *Immunity*, 2019, **51**, 27–41.
8 R. Medzhitov, *Cell*, 2010, **140**, 771–776.
9 L. Wu, S. Saxena, M. Awaji and R. K. Singh, *Cancers*, 2019, **11**, 564.
10 T. S. Ibrahim, A. M. Malebari and M. F. A. Mohamed, *Pharmaceuticals*, 2021, **14**, 1177.
11 A. Mantovani, P. Allavena, A. Sica and F. Balkwill, *Nature*, 2008, **454**, 436–444.
12 P. Igor, K. Katarzyna and S. Wiktoria, *Rep. Pract. Oncol. Radiother.*, 2020, **35**(3), 422–427.
13 B. L. Sng and S. A. Schug, *Ann. Acad. Med. Singapore*, 2009, **38**, 960–966.
14 X. Y. Sun, C. Hu, X. Q. Deng, C. X. Wei, Z. G. Sun and Z. S. Quan, *Eur. J. Med. Chem.*, 2010, **45**, 4807–4812.
15 R. Eccles, *J. Clin. Pharm. Ther.*, 2006, **31**, 309–319.
16 A. M. Mohassab, H. A. Hassan, D. Abdelhamid, M. Abdel-Aziz, K. N. Dalby and T. S. Kaoud, *Bioorg. Chem.*, 2017, **75**, 242–259.
17 M. F. A. Mohamed, A. A. Marzouk, A. Nafady, D. A. El-Gamal, R. M. Allam, G. E.-D. A. Abuo-Rahma, H. I. El Subbagh and A. H. Moustafa, *Bioorg. Chem.*, 2020, **105**, 104439.
18 H. Kakuta, X. Zheng, H. Oda, S. Harada, Y. Sugimoto, K. Sasaki and A. Tai, *J. Med. Chem.*, 2008, **51**, 2400–2411.
19 M. G. Perrone, D. D. Lofrumento, P. Vitale, F. De Nuccio, V. La Pesa, A. Panella, R. Calvello, A. Cianciulli, M. A. Panaro and A. Scilimati, *Pharmacology*, 2015, **95**, 22–28.
20 B. G. M. Youssif, M. F. A. Mohamed, M. M. Al-Sanea, A. H. Moustafa, A. A. Abdelhamid and H. A. M. Gomaa, *Bioorg. Chem.*, 2019, **85**, 577–584.
21 K. M. Lim, J. Y. Lee, S. M. Lee, O. N. Bae, J. Y. Noh, E. J. Kim, S. M. Chung and J. H. Chung, *Br. J. Pharmacol.*, 2009, **156**, 328–337.
22 L. Ma, C. Xie, Y. Ma, J. Liu, M. Xiang, X. Ye, H. Zheng, Z. Chen, Q. Xu, T. Chen, J. Chen, J. Yang, N. Qiu, G. Wang, X. Liang, A. Peng, S. Yang, Y. Wei and L. Chen, *J. Med. Chem.*, 2011, **54**, 2060–2068.
23 A. H. Abdelazeem, S. A. Abdelatef, M. T. El-Saadi, H. A. Omar, S. I. Khan, C. R. McCurdy and S. M. El-Moghazy, *Eur. J. Pharm. Sci.*, 2014, **62**, 197–211.
24 F. Colotta, P. Allavena, A. Sica, C. Garlanda and A. Mantovani, *Carcinogenesis*, 2009, **30**, 1073–1081.
25 E. Vitaku, D. T. Smith and J. T. Njardarson, *J. Med. Chem.*, 2014, **57**, 10257–10274.
26 M. Montana, V. Montero, O. Khoumeri and P. Vanelle, *Molecules*, 2021, **26**, 4742.
27 S. A. Khan, K. Saleem and Z. Khan, *Eur. J. Med. Chem.*, 2007, **42**, 103–108.
28 S. K. Suthar, N. S. Chundawat, G. Pal Singh, J. M. Padrón and Y. Kunwar Jhala, *Eur. J. Med. Chem. Rep.*, 2022, 100040, DOI: **10.1016/j.ejmcr.2022.100040**.
29 J. A. Pereira, A. M. Pessoa, M. N. D. S. Cordeiro, R. Fernandes, C. Prudêncio, J. P. Noronha and M. Vieira, *Eur. J. Med. Chem.*, 2015, **97**, 664–672.
30 D. K. Kölmel and E. T. Kool, *Chem. Rev.*, 2017, **117**, 10358–10376.
31 H. Gao, E. F. Yamasaki, K. K. Chan, L. L. Shen and R. M. Snapka, *Cancer Res.*, 2000, **60**, 5937–5940.
32 T. Uehara, Y. Minoshima, K. Sagane, N. H. Sugi, K. O. Mitsuhashi, N. Yamamoto, H. Kamiyama, K. Takahashi, Y. Kotake, M. Uesugi, A. Yokoi, A. Inoue, T. Yoshida, M. Mabuchi, A. Tanaka and T. Owa, *Nat. Chem. Biol.*, 2017, **13**, 675–680.
33 H. Gao, K. C. Huang, E. F. Yamasaki, K. K. Chan, L. Chohan and R. M. Snapka, *Proc. Natl. Acad. Sci. U. S. A.*, 1999, **96**, 12168–12173.
34 S. D. Undevia, F. Innocenti, J. Ramirez, L. House, A. A. Desai, L. A. Skoog, D. A. Singh, T. Karrison, H. L. Kindler and M. J. Ratain, *Eur. J. Cancer*, 2008, **44**, 1684–1692.
35 M. Liu, Y. Wang, W.-z. Wangyang, F. Liu, Y.-l. Cui, Y.-s. Duan, M. Wang, S.-z. Liu and C.-h. Rui, *J. Agric. Food Chem.*, 2010, **58**, 6858–6863.
36 S. Rollas and S. G. Küçükgüzel, *Molecules*, 2007, **12**, 1910–1939.

37 G. Verma, A. Marella, M. Shaquiquzzaman, M. Akhtar, M. R. Ali and M. M. Alam, *J. Pharm. BioAllied Sci.*, 2014, **6**, 69–80.
38 N. Radhoff and A. Studer, *Chem. Sci.*, 2022, **13**, 3875–3879.
39 I. Khan, S. Zaib and A. Ibrar, *Org. Chem. Front.*, 2020, **7**, 3734–3791.
40 Y.-C. Zhang, F. Jiang and F. Shi, *Acc. Chem. Res.*, 2020, **53**, 425–446.
41 E. A. Ahmed, M. F. A. Mohamed, A. Omran and H. Salah, *Synth. Commun.*, 2020, **50**, 2924–2940.
42 N. A. Qandeel, A. K. El-Damasy, M. H. Sharawy, S. M. Bayomi and N. S. El-Gohary, *Bioorg. Chem.*, 2020, **102**, 103890.
43 T. S. Ibrahim, A. M. Malebari and M. F. A. Mohamed, *Pharmaceuticals*, 2021, **14**, 1177.
44 H. A. Abou-Zied, B. G. M. Youssif, M. F. A. Mohamed, A. M. Hayallah and M. Abdel-Aziz, *Bioorg. Chem.*, 2019, **89**, 102997.
45 B. J. Aungst, *J. Pharm. Sci.*, 2017, **106**, 921–929.
46 M. F. Mohamed, A. A. Marzouk, A. Nafady, D. A. El-Gamal, R. M. Allam, G. A. Abuo-Rahma, H. I. El Subbagh and A. H. Moustafa, *Bioorg. Chem.*, 2020, 104439.
47 C. A. Lipinski, F. Lombardo, B. W. Dominy and P. J. Feeney, *Adv. Drug Delivery Rev.*, 2001, **46**, 3–26.
48 M. A. Bakht, M. S. Yar, S. G. Abdel-Hamid, S. I. Al Qasoumi and A. Samad, *Eur. J. Med. Chem.*, 2010, **45**, 5862–5869.
49 D. F. Veber, S. R. Johnson, H. Y. Cheng, B. R. Smith, K. W. Ward and K. D. Kopple, *J. Med. Chem.*, 2002, **45**, 2615–2623.
50 M. J. Uddin, P. N. P. Rao and E. E. Knaus, *Bioorg. Med. Chem.*, 2004, **12**, 5929–5940.
51 M. A. A. El-Sayed, N. I. Abdel-Aziz, A. A. M. Abdel-Aziz, A. S. El-Azab, Y. A. Asiri and K. E. H. ElTahir, *Bioorg. Med. Chem.*, 2011, **19**, 3416–3424.